

Simple co-precipitation synthesis of high-voltage spinel cathodes with different Ni/Mn ratios for lithium-ion batteries

Yuan Xue · Li-Li Zheng · Zhen-Bo Wang · Yi Han · Fu-Da Yu · Yu-Xiang Zhou

Received: 29 May 2018 / Accepted: 10 September 2018 / Published online: 19 September 2018
© Springer Nature B.V. 2018

Abstract The high-voltage spinel is a promising cathode material in next generation of lithium-ion batteries. Samples $\text{LiNi}_{0.5-x}\text{Mn}_{1.5+x}\text{O}_4$ ($x = 0, 0.05, 0.1$) are synthesized by a simple co-precipitation method, in which pH value and temperature conditions do not need control. In the simple co-precipitation method, NaHCO_3 solution is poured into transition metal solution to produce precursor. Ni and Mn are distributed uniformly in the products. The as-prepared samples are composed of ~200 nm primary particles. Samples $\text{LiNi}_{0.5-x}\text{Mn}_{1.5+x}\text{O}_4$ ($x = 0, 0.05, 0.1$) are also tested to study the effects of different Ni/Mn ratios. Sample $\text{LiNi}_{0.5}\text{Mn}_{1.5}\text{O}_4$ delivers discharge capacities of 130 mAh g^{-1} at 0.2 C. The decreasing of Ni/Mn ratio in samples reduces specific capacity. With the decreasing of Ni/Mn ratios in spinel, amount of Mn^{3+} are increased. Attributed to its high Mn^{3+} contents, sample $\text{LiNi}_{0.4}\text{Mn}_{1.6}\text{O}_4$ delivers the highest discharge capacity of 106 mAh g^{-1} at a large current density of 15 C, keeping 84.5% of that at 0.2 C rate. With the increasing of Ni/Mn ratios in spinel, cycling performance is improved. Sample $\text{LiNi}_{0.5}\text{Mn}_{1.5}\text{O}_4$ shows the best cycling stability, keeping 94.4% and 90.4% of the highest discharge capacities after 500 cycles at 1 C and 1000 cycles at 5 C.

Keywords Cathode material · Co-precipitation · Ni/Mn ratio · $\text{LiNi}_{0.5}\text{Mn}_{1.5}\text{O}_4$ · High voltage · Energy storage

Introduction

Energy crisis and greenhouse gas emission have brought unprecedented attention all over the world. High energy and high power rechargeable lithium-ion batteries are the most promising energy storage systems for electric vehicles and plug-in hybrids. The development of those systems is in need of battery with higher energy density and longer life (Goodenough 2014; Croguennec and Palacin 2015; Cai et al. 2014, 2015, 2016; Zhang et al. 2018; Fang et al. 2017). $\text{LiNi}_{0.5}\text{Mn}_{1.5}\text{O}_4$ has caused great interests as high-voltage cathode material (Santhanam and Rambabu 2010; Manthiram et al. 2014; Yi et al. 2016; Kim et al. 2004). $\text{LiNi}_{0.5}\text{Mn}_{1.5}\text{O}_4$ has a high theoretical energy density above 600 Wh kg^{-1} because of its high specific capacity (147 mAh g^{-1}) and high potential plateau (4.7 V). Besides, the facial three-dimensional lithium-ion diffusion pathways of $\text{LiNi}_{0.5}\text{Mn}_{1.5}\text{O}_4$ give rise to its high power density.

The synthesis methods of $\text{LiNi}_{0.5}\text{Mn}_{1.5}\text{O}_4$ mainly include wet chemical reaction and solid-state method. Solid-state method (Lv et al. 2014; Zhu et al. 2013) is used because of its simplification and low cost. But in this method, it is difficult to achieve the even mix of Mn and Ni elements. Wet chemical methods include co-precipitation methods, sol-gel methods (Li and Li 2014; Bauer et al. 2015), and hydrothermal methods

Yuan Xue and Li-Li Zheng contributed equally to this work.

Y. Xue · L.-L. Zheng · Z.-B. Wang (✉) · Y. Han · F.-D. Yu · Y.-X. Zhou

MIT Key Laboratory of Critical Materials Technology for New Energy Conversion and Storage, School of Chemistry and Chemical Engineering, Harbin Institute of Technology, No. 92 West-Da Zhi Street, Harbin 150001, China
e-mail: wangzhib@hit.edu.cn

(Xue et al. 2014). The co-precipitation method has been reported by many groups (Luo 2015; Yao et al. 2014, Zhang et al. 2012; Gu et al. 2014, 2015; Chemelewski et al. 2013; Liu et al. 2013a, b; Li et al. 2013; Axmann et al. 2016; Liu et al. 2015). Its main advantage is homogeneously mixing Ni and Mn. However, traditional co-precipitation procedure is very inconvenient and complex. Because pH value and temperature conditions of the solution must be controlled precisely to produce precursor using a continuously stirred tank reactor (CSTR). And ammonia is usually used as complexing agent. There are two main systems: hydroxide and carbonate. In hydroxide co-precipitation method, pH is controlled at about 10 with NaOH as precipitant. And argon serves as a shielding gas to protect Mn from oxidation. In carbonate co-precipitation method, pH is controlled at about 8 with Na_2CO_3 as precipitant. If pH value of solution is too high, transition metal carbonate precipitate will turn into hydroxide precipitate.

Herein, samples $\text{LiNi}_{0.5-x}\text{Mn}_{1.5+x}\text{O}_4$ ($x = 0, 0.05,$ and 0.1) are prepared by the simple co-precipitation, in which temperature and pH conditions do not need control. And LNMO materials synthesized by the simple co-precipitation method show better electrochemical performance than those of traditional co-precipitation methods. Besides, Ni/Mn ratios in LNMO materials are of great importance to the performances (Wan et al. 2015; Ren et al. 2014; Song et al. 2012). Different Ni/Mn ratios can change the Mn^{3+} contents in spinel, leading to different electrochemical performances. Here, the effects of different Ni/Mn ratios in spinel are studied in detail.

Experimental

Preparation of LNMO

A NaHCO_3 solution (0.4 mol L^{-1}) was poured to the NiSO_4 and MnSO_4 solution rapidly under stirring. The molar ratios of NiSO_4 and MnSO_4 are 0.5:1.5, 0.45:1.55, and 0.4:1.6, respectively. The total concentration is 0.04 mol L^{-1} . The mixture was kept stirring for 5 h. Then, the produced precipitate was collected, washed, and dried. The precipitate and $\text{LiOH}\cdot\text{H}_2\text{O}$ were dispersed in ethanol and stirred. The ethanol was evaporated under stirring. The obtained mixture was calcined at $800 \text{ }^\circ\text{C}$ for 12 h in air to obtain $\text{LiNi}_{0.5}\text{Mn}_{1.5}\text{O}_4$, $\text{LiNi}_{0.45}\text{Mn}_{1.55}\text{O}_4$, and

$\text{LiNi}_{0.4}\text{Mn}_{1.6}\text{O}_4$ powder, denoted as samples Ni0.5, Ni0.45, and Ni0.4, respectively.

Characterization

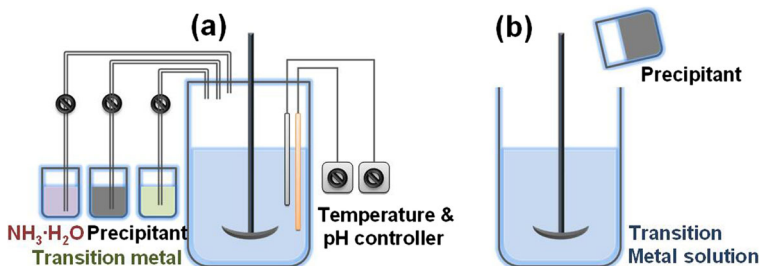
Scanning electron microscopy (SEM, Quanta-200) and transmission electron microscopy (TEM, FEI Tecnai-F30FEG) were used to analyze morphology and microstructure of the as-prepared materials. Inductively coupled plasma (ICP, PerkinElmer, Optima 5300DV) was used to analyze Ni/Mn ratios. X-ray powder diffraction analysis was carried out with a D/max-RB diffractometer using a $\text{Cu K}\alpha$ source and recorded with a step of 0.05° .

The 2025 coin cells were assembly in a pure argon-filled glove box. To make the working electrode, 80 wt% active material, 10 wt% conductive acetylene black as conductive agent, and 10 wt% polyvinylidene fluoride as binder with proper amount of *n*-methyl pyrrolidinone (NMP) as a solvent were put on a piece of aluminum foil. After drying in a vacuum oven at $120 \text{ }^\circ\text{C}$, the foil was punched into a circular electrode. The loading weight of the cathode active material was about 3 mg cm^{-2} . Lithium metal was used as anode in the cell. Charge and discharge tests were carried out on a battery testing system (NEWWARE BTS 5 V 10 mA) between 3.5 and 4.95 V. If the current density was higher than 0.2 C, the cells were charged galvanostatically to 4.95 V first and kept at 4.95 V until the current decreased to 0.1 C.

Results and discussion

Co-precipitation methods have been widely used to synthesize LNMO materials. Precipitate is generated simultaneously and Ni/Mn elements distribute uniformly in co-precipitation procedure. However, traditional co-precipitation procedure is very inconvenient and complex. Here, precursors are synthesized by a simple co-precipitation method, in which NaHCO_3 solution is poured into transition metal solution rapidly. Traditional co-precipitation methods (Luo 2015; Yao et al. 2014; Zhang et al. 2012; Gu et al. 2014, 2015; Chemelewski et al. 2013; Liu et al. 2013a, b; Li et al. 2013; Axmann et al. 2016; Liu et al. 2015) and simple co-precipitation method used in this work are compared in Scheme 1 and Table 1. During the simple co-precipitation procedure, temperature, and pH conditions of solution do not need

Scheme 1 Illustration of **a** traditional co-precipitation procedure and **b** simple co-precipitation method



control attributed to the following reasons. Complexing agent ammonia is not added, so transition metal cannot complex with NH_3 and can be precipitated completely. In the simple co-precipitation procedure, NaHCO_3 is used as precipitant instead of Na_2CO_3 and NaOH . The pH value of NaHCO_3 solution is about 8.3, avoiding hydroxide precipitate. The NaHCO_3 solution is poured, not dropped, into transition metal solution rapidly. So, transition metal can generate precipitate immediately and simultaneously. Moreover, LNMO materials synthesized using the simple co-precipitation method show better electrochemical performance than those of traditional co-precipitation methods, as shown in Table 1.

To study the effects of different Ni/Mn ratios, samples $\text{LiNi}_{0.5}\text{Mn}_{1.5}\text{O}_4$, $\text{LiNi}_{0.45}\text{Mn}_{1.55}\text{O}_4$, and $\text{LiNi}_{0.4}\text{Mn}_{1.6}\text{O}_4$, denoted as Ni0.5, Ni0.45, and Ni0.4, are prepared by the simple co-precipitation method. The ICP is used to test the molar ratios of Ni/Mn in the samples. The ICP results show that the molar ratios of Ni/Mn in Ni0.5, Ni0.45, and Ni0.4 are 0.50/1.50, 0.44/1.56, and 0.39/1.61, close to the designed formulas in this work.

Figure 1a shows the XRD patterns of transition metal carbonate obtained after co-precipitation process. Peak positions of the three patterns are the same and the XRD patterns can be assigned to the rhombohedral structure of MnCO_3 (JCPDS Card No.: 83-1763). Peak intensities of all precursors are low because they are obtained without calcination. Figure 1b shows the SEM images of $\text{Ni}_{0.5}\text{Mn}_{1.5}(\text{CO}_3)_2$. As can be seen, the obtained transition metal carbonate precursors are microspheres.

XRD patterns of LNMO samples are displayed in Fig. 2. The XRD patterns of all powders are representative of cubic spinel (JCPDS Card No.: 80-2162). Minor peaks at 37.5° , 43.6° , and 63.4° related to $\text{Li}_x\text{Ni}_{1-x}\text{O}$ impurity (Song et al. 2012; Liu et al. 2013a, b) are not observed in these patterns. It means that LNMO samples have very little impurity, beneficial for performance of LNMO (Yi and Hu 2007). The superstructure reflection at 15.3° is typical for an ordered LNMO (Axmann et al. 2016; Lee et al. 2012). The peak intensity at 15.3° of sample Ni0.4

Table 1 Comparison of preparation conditions and electrochemical performance of LNMO (“-” means that the data is not reported)

Precipitant	Complex agent	pH	Temperature/ °C	Capacity/ mAh g^{-1}	Cycle stability	Rate capability/ mAh g^{-1}	Ref.
NaHCO_3	None	No control	Room temp.	130	1 C 500th, 94% 5 C 1000th, 90%	110 at 10 C 99 at 15 C	Our work
Na_2CO_3	$\text{NH}_3 \cdot \text{H}_2\text{O}$	8.0	60	128	1 C 50th, 98%	104 at 10 C	Luo 2015
Na_2CO_3	$\text{NH}_3 \cdot \text{H}_2\text{O}$	7~8	55	115	1 C 50th, 96%	96 at 2 C	Yao et al. 2014
Na_2CO_3	$\text{NH}_3 \cdot \text{H}_2\text{O}$	7.8	60	142	1 C 50th, 97%	127 at 2 C	Zhang et al. 2012
Na_2CO_3	$\text{NH}_3 \cdot \text{H}_2\text{O}$	8.3	55	128	-	-	Gu et al. 2014
Na_2CO_3	$\text{NH}_3 \cdot \text{H}_2\text{O}$	8.3	55	126	-	-	Gu et al. 2015
NaOH	$\text{NH}_3 \cdot \text{H}_2\text{O}$	10	60	133	0.2 C 100th, 94%	116 at 10 C	Chemelewski et al. 2013
NaOH	$\text{NH}_3 \cdot \text{H}_2\text{O}$	10.5	-	131	1 C 100th, 93%	-	Liu et al. 2013a, b
NaOH	$\text{NH}_3 \cdot \text{H}_2\text{O}$	10.2	60	135	-	-	Li et al. 2013
NaOH	$\text{NH}_3 \cdot \text{H}_2\text{O}$	-	-	131	-	115 at 5 C	Axmann et al. 2016
$\text{H}_2\text{C}_2\text{O}_4$	$\text{NH}_3 \cdot \text{H}_2\text{O}$	8	50	140	0.2 C 50th, 98%	106 at 10 C	Liu et al. 2015

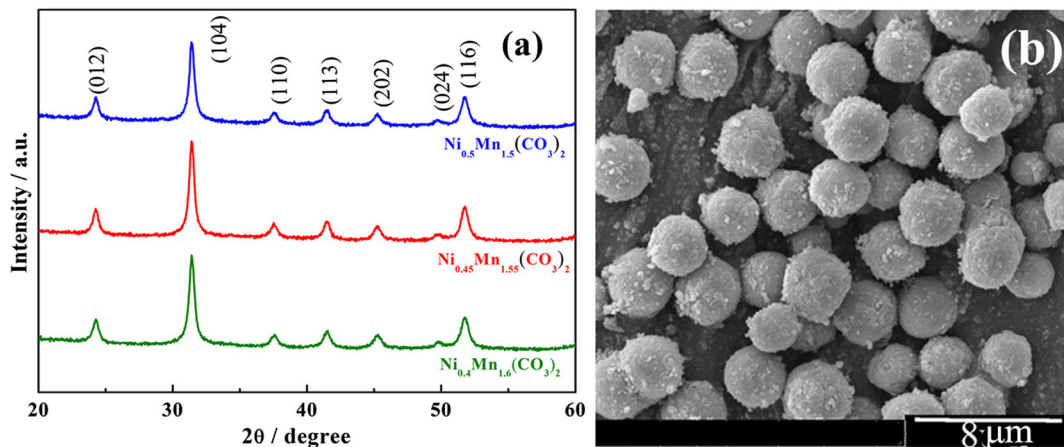


Fig. 1 a XRD patterns and b SEM micrographs of precursors

is the strongest, meaning that sample Ni0.4a has the highest level of cation ordering.

The morphologies and structures of different LNMO samples were investigated by TEM and SEM as shown in Fig. 3. The SEM images with low magnification are shown in Fig. 3k. All samples are consisted of spherical particles with uniform dispersion. The particle sizes of Ni0.5, Ni0.45, and Ni0.4 are about 4.1, 3.0, and 2.2 μm , respectively. Solubility product constant of NiCO_3 and MnCO_3 are 6.6×10^{-9} and 2.2×10^{-11} . MnCO_3 is more easily to be precipitated. Nucleation rate is increased with the decreasing of Ni/Mn ratios, leading to small LNMO particle size. SEM images with higher magnitude are shown as Fig. 3d–f. The LNMO particles are composed of $\sim 200\text{-nm}$ primary particles. EDS mapping of sample Ni0.45 are shown in Fig. 3g–i. Mn and Ni are distributed uniformly in particles, meaning that the simple co-precipitation method can mix Mn and Ni

homogeneously. The EDS results show that the atomic ratios of Ni/Mn in Ni0.5, Ni0.45, and Ni0.4 are 0.49/1.51, 0.42/1.58, and 0.38/1.62. As shown in Fig. 3l, LNMO samples have hollow structures. The hollow structures may be caused by Ostwald ripening during calcining process (Xue et al. 2017). The hollow structures are beneficial for electrochemical performance. The hollow structures can reduce Li^+ ions transport path, leading to good rate performance. Besides, the hollow structures can buffer the volume change caused by Li^+ insertion/extraction, which are helpful to improve cycling performance (Fang et al. 2018; Tong et al. 2018). The spinel crystal structure of LNMO is further confirmed by the high-resolution TEM images as shown in Fig. 3m, n, in which the interplanar spacing is consistent with the (111) atomic planes.

The electrochemical performances of LNMO samples were tested in coin cells with lithium metal as

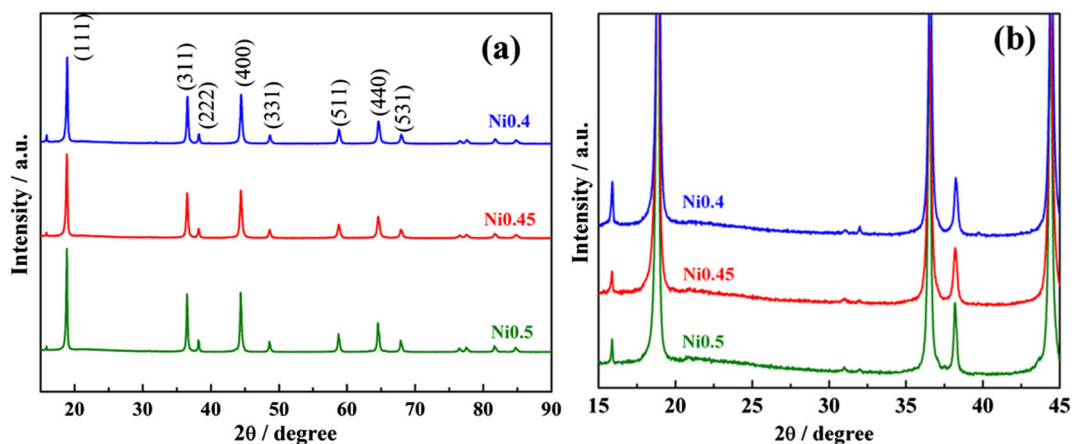


Fig. 2 a XRD patterns and b magnified XRD patterns of LNMO samples

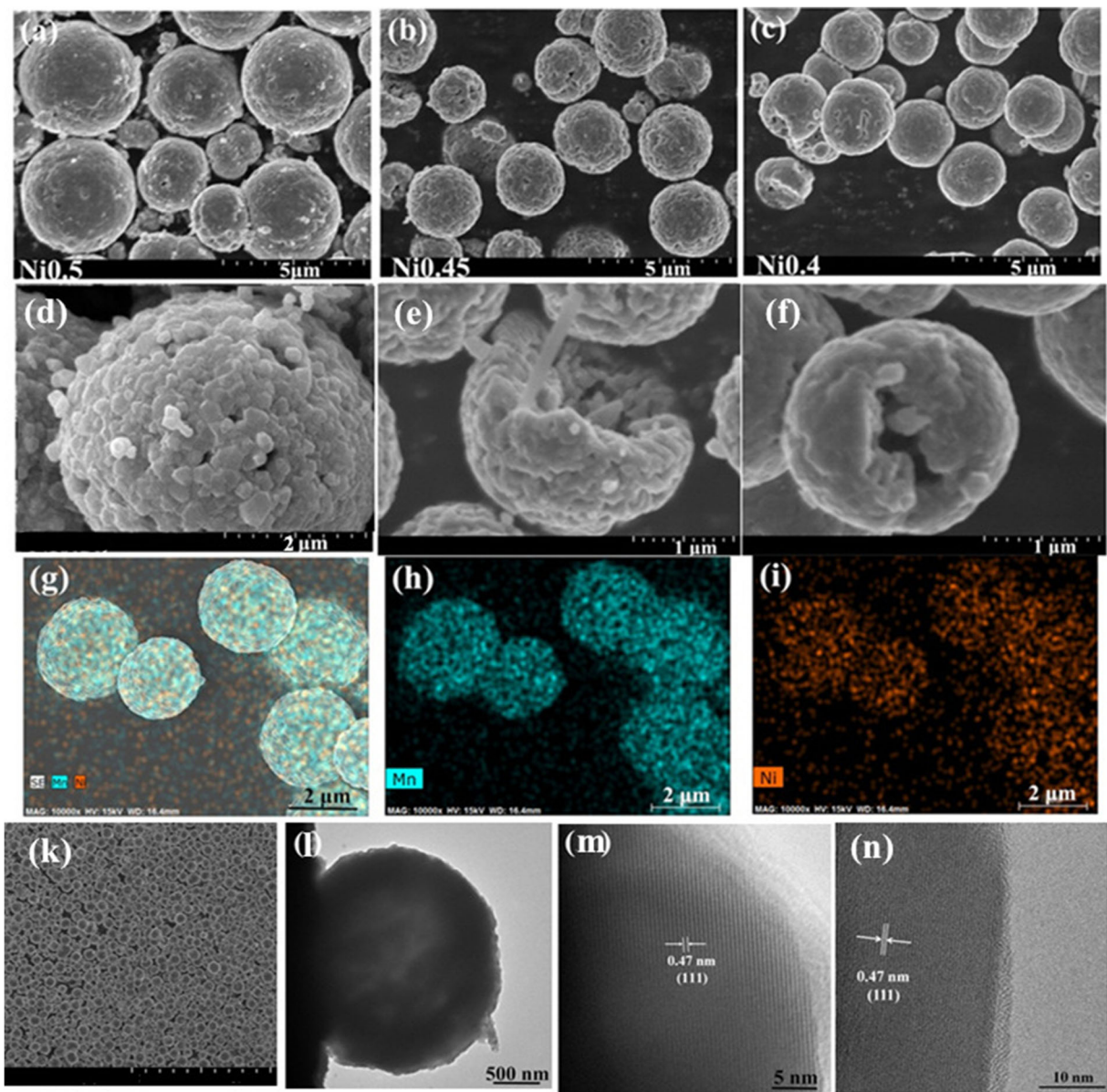


Fig. 3 SEM micrographs of sample **a, d** Ni_{0.5}, **b, e** Ni_{0.45}, **c, f** Ni_{0.4}, **g–i** EDS mapping of Ni_{0.45}, **k** low-magnification SEM image, and **l–n** TEM micrographs of sample Ni_{0.45}

anode. The charge-discharge curves of 0.2 C are showed in Fig. 4. The capacities of LNMO are mainly generated from Ni⁴⁺/Ni²⁺ redox. So, the decreases of Ni/Mn ratios in samples reduce specific capacities. The specific discharge capacities of Ni_{0.5}, Ni_{0.45}, and Ni_{0.4} are 130, 127, and 122 mAh g⁻¹, respectively. All samples show two distinct discharge plateaus at ~4.7 V, attributed to the reduction of Ni⁴⁺ to Ni³⁺ and Ni³⁺ to Ni²⁺, respectively (Lee et al. 2012; Kunduraci and Amatucci 2007). Sample Ni_{0.4} shows larger voltage gap between the two

plateaus at ~4.7 V due to its high level of cation ordering, as showed in the insert in Fig. 4 (Kunduraci and Amatucci 2007). A minor plateau in 4-V region is also observable, which originates from the reduction of Mn⁴⁺ to Mn³⁺ due to the presence of small amount of Mn³⁺ (Kunduraci and Amatucci 2006). The length of 4-V plateau in discharging curve can be used to calculate the relative amount of Mn³⁺ ions in LNMO (Xiao et al. 2012; Moorhead-Rosenberg et al. 2012). Therefore, the capacity percentages were calculated from the capacity

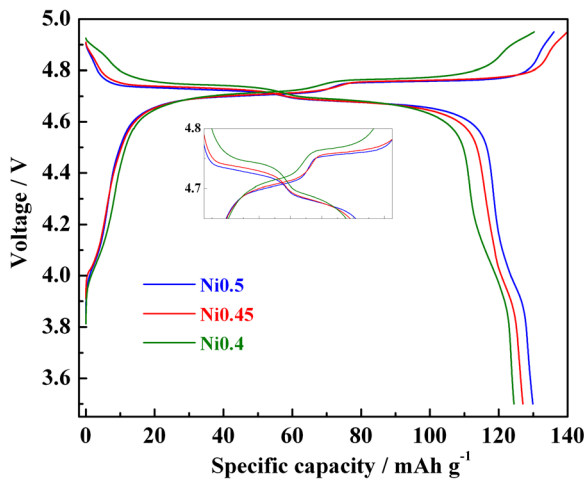


Fig. 4 Charge and discharge capacity curves at 0.2 C of LNMO samples

between 3.8 and 4.2 V divided by the total discharge capacity to evaluate the amount of Mn^{3+} ions in spinel. The capacity percentages of 4 V plateau of Ni0.5, Ni0.45, and Ni0.4 are 5.4%, 6.0% and 8.5%, respectively. The amount of Mn^{3+} increases with the decreasing of Ni/Mn ratios. This is because part of Mn is reduced to 3+ to keep charge neutrality in materials.

Cyclic voltammetry is tested to study the oxidation/reduction behavior of LNMO samples as shown in Fig. 5. Samples show similar main peaks at 4.7 V ascribed to the $\text{Ni}^{2+}/\text{Ni}^{4+}$ redox couple. As shown, the gap between the oxidation peak and reduction peak of sample Ni0.4 is smaller than the others, implying good electrochemical reversibility. Besides, the small peaks at around 4.0 V are related to the $\text{Mn}^{3+}/\text{Mn}^{4+}$ redox couple.

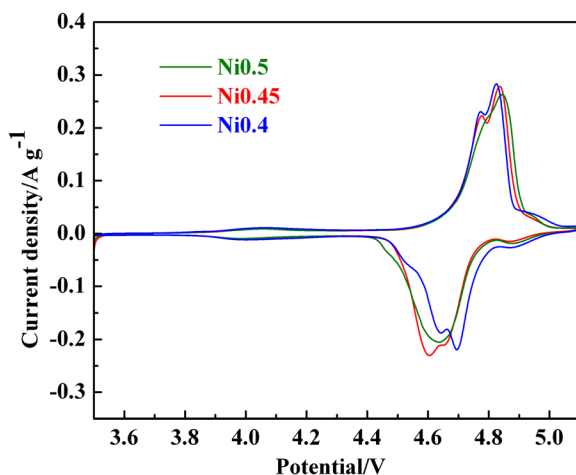


Fig. 5 Cyclic voltammetry curves of LNMO samples

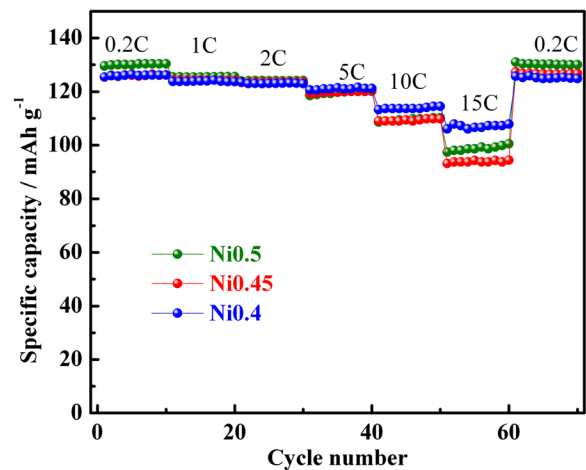


Fig. 6 Rate capacity of LNMO samples

To evaluate the rate capabilities of the materials, the cells were cycled at current densities from 0.2 to 15 C. Figure 6 shows the specific capacities at different discharge rates. The discharge capacities decrease as the current density increases. At 15-C rate, sample Ni0.4 delivers discharge capacity of 106.1 mAh g^{-1} , reaching 84.5% of that at 0.2-C rate, higher than 75.1% and 73.8% of Ni0.5 and Ni0.45. The best rate performance of Ni0.4 sample is attributed to its highest Mn^{3+} content. With the presence of Mn^{3+} , samples have higher electronic and lithium-ion conductivity (Xiao et al. 2013; Kunduraci et al. 2006).

Then, the cycling performance of LNMO was tested at 1 C for 500 cycles and 5 C for 1000 cycles as shown in Fig. 7. With the increasing of Ni/Mn ratios in spinel, their cycling performances are improved. Sample Ni0.5 shows the best cycling stability, keeping 94.4% and 90.4% of the highest discharge capacities after 500 cycles at 1 C and 1000 cycles at 5C. It is better than other recent report $\text{LiNi}_{0.5}\text{Mn}_{1.5}\text{O}_4$ (Yin et al. 2018; Mou et al. 2018). The Mn^{3+} ion in LNMO tends to undergo a disproportionation reaction. The produced Mn^{2+} ion dissolves into the electrolyte, leading to a capacity fading during cycling (Park et al. 2011; Pieczonka et al. 2013). So, with the lowest Mn^{3+} contents, sample Ni0.5 shows the best cycling performance.

Conclusions

Samples $\text{LiNi}_{0.5-x}\text{Mn}_{1.5+x}\text{O}_4$ ($x = 0, 0.05, 0.1$) are synthesized by the simple co-precipitation method, in which NaHCO_3 solution is poured into transition metal

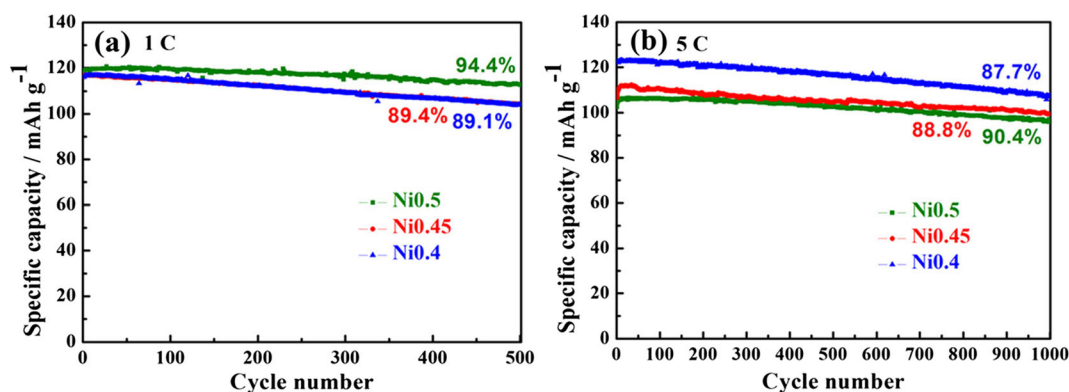


Fig. 7 Cycling performances at different current densities of **a** 1 C and **b** 5 C of LNMO samples

solution rapidly to produce precursor. It is very simple that temperature and pH conditions do not need control. With the decreasing of Ni/Mn ratios in spinel, their specific capacities are reduced and amount of Mn^{3+} is increased. Sample $\text{LiNi}_{0.4}\text{Mn}_{1.6}\text{O}_4$ shows the best rate performance attributed to its high Mn^{3+} contents, which delivers a high discharge capacity of 106 mAh g^{-1} at 15 C, keeping 84.5% of that at 0.2 C rate. Cycling performance of sample is improved with the increasing Ni/Mn ratios in spinel. Sample $\text{LiNi}_{0.5}\text{Mn}_{1.5}\text{O}_4$ shows the best cycling stability, keeping 94.4% and 90.4% of the highest discharge capacities after 500 cycles at 1 C and 1000 cycles at 5 C.

Acknowledgements We acknowledge the National Natural Science Foundation of China (Grant Nos. 21273058 and 21673064), China postdoctoral science foundation (Grant Nos. 2017M621285 and 2018T110292), and Harbin technological achievements transformation projects (2016DB4AG023) for their financial support.

Compliance with ethical standards

Conflict of interest The authors declare that they have no conflict of interest.

References

- Axmann P, Gabrielli G, Wohlfahrt-Mehrens M (2016) Tailoring high-voltage and high-performance $\text{LiNi}_{0.5}\text{Mn}_{1.5}\text{O}_4$ cathode material for high energy lithium-ion batteries. *J Power Sources* 301:151–159
- Bauer S, Biasi L, Glatthaar S, Toukam L, Geßwein H, Baumbach T (2015) In operando study of the high voltage spinel cathode material $\text{LiNi}_{0.5}\text{Mn}_{1.5}\text{O}_4$ using two dimensional full-field spectroscopic imaging of Ni and Mn. *Phys Chem Chem Phys* 17:16388–16397
- Cai Y, Huang Y, Wang X, Jia D, Tang X (2014) Long cycle life, high rate capability of truncated octahedral LiMn_2O_4 cathode materials synthesized by a solid-state combustion reaction for lithium ion batteries. *Ceram Int* 40:14039–14043
- Cai Y, Huang Y, Wang X, Cai D, Jia W, Tang X (2015) Facile synthesis of LiMn_2O_4 octahedral nanoparticles as cathode materials for high capacity lithium ion batteries with long cycle life. *J Power Sources* 278:574–581
- Cai Y, Huang Y, Jia W, Wang X, Guo Y, Jia D, Guo Z (2016) Super high-rate, long cycle life of europium-modified, carbon-coated, hierarchical mesoporous lithium-titanate anode materials for lithium ion batteries. *J Mater Chem A* 4:9949–9957
- Chemelewski KR, Shin DW, Li W, Manthiram A (2013) Octahedral and truncated high-voltage spinel cathodes: the role of morphology and surface planes in electrochemical properties. *J Mater Chem A* 1:3347
- Croguennec L, Palacin MR (2015) Recent achievements on inorganic electrode materials for lithium-ion batteries. *J Am Chem Soc* 137:3140–3156
- Fang Y, Huang Y, Zhang S, Jia W, Wang X, Guo Y, Wang L (2017) Synthesis of unique hierarchical mesoporous layered-cube Mn_2O_3 by dual-solvent for high-capacity anode material of lithium-ion batteries. *Chem Eng J* 315:583–590
- Fang Y, Huang Y, Tong W, Cai Y, Wang X, Guo Y, Zong J (2018) Synthesis of hollow peanut-like hierarchical mesoporous $\text{LiNi}_{1/3}\text{Co}_{1/3}\text{Mn}_{1/3}\text{O}_2$ cathode materials with exceptional cycle performance for lithium-ion batteries by a simple self-template solid-state method. *J Alloys Compd* 743:707–715
- Goodenough JB (2014) Electrochemical energy storage in a sustainable modern society. *Energy Environ Sci* 7:14–18
- Gu YJ, Zang QF, Liu HQ, Ding JX, Wang YM, Wang HF, Wei WG (2014) Characterization and electrochemical properties of $\text{LiNi}_{0.5}\text{Mn}_{1.5}\text{O}_4$ prepared by a carbonate co-precipitation method. *Int J Electrochem Sci* 9:1
- Gu YJ, Li Y, Fu Y, Zang QF, Liu HQ, Ding JX, Ni J (2015) $\text{LiNi}_{0.5}\text{Mn}_{1.5}\text{O}_4$ synthesized through ammonia-mediated carbonate precipitation. *Electrochim Acta* 176:1029–1035
- Kim JH, Myung ST, Yoon CS, Kang SG, Sun YK (2004) Comparative study of $\text{LiNi}_{0.5}\text{Mn}_{1.5}\text{O}_{4-\delta}$ and $\text{LiNi}_{0.5}\text{Mn}_{1.5}\text{O}_4$ cathodes having two crystallographic structures: Fd3m and P4₃32. *Chem Mater* 16:906
- Kunduraci M, Amatucci GG (2006) Synthesis and characterization of nanostructured 4.7 V $\text{Li}_x\text{Mn}_{1.5}\text{Ni}_{0.5}\text{O}_4$ spinels for

- high-power lithium-ion batteries. *J Electrochem Soc* 153: A1345
- Kunduraci M, Amatucci GG (2007) Effect of oxygen non-stoichiometry and temperature on cation ordering in $\text{LiMn}_{2-x}\text{Ni}_x\text{O}_4$ ($0.50 \geq x \geq 0.36$) spinels. *J Power Sources* 165:359–367
- Kunduraci M, Al-sharab JF, Amatucci GG (2006) High-power nanostructured $\text{LiMn}_{2-x}\text{Ni}_x\text{O}_4$ high-voltage lithium-ion battery electrode materials: electrochemical impact of electronic conductivity and morphology. *Chem Mater* 18:3585–3592
- Lee ES, Nam KW, Hun E, Manthiram A (2012) Influence of cation ordering and lattice distortion on the charge–discharge behavior of $\text{LiNi}_{0.5}\text{Mn}_{1.5}\text{O}_4$ spinel between 5.0 and 2.0 V. *Chem Mater* 24:3610
- Li XP, Li WS (2014) Crystallographic facet-and size-controllable synthesis of spinel $\text{LiNi}_{0.5}\text{Mn}_{1.5}\text{O}_4$ with excellent cyclic stability as cathode of high voltage lithium ion battery. *J Mater Chem A* 2:11987
- Li SR, Chen CH, Camardese J, Dahn JR (2013) High precision coulometry study of $\text{LiNi}_{0.5}\text{Mn}_{1.5}\text{O}_4/\text{Li}$ coin cells. *J Electrochem Soc* 160:A1517–A1523
- Liu G, Park KS, Song J, Goodenough JB (2013a) Influence of thermal history on the electrochemical properties of $\text{Li}[\text{Ni}_{0.5}\text{Mn}_{1.5}]\text{O}_4$. *J Power Sources* 243:260
- Liu J, Sun Z, Xie J, Chen H, Wu N, Wu B (2013b) Synthesis and electrochemical properties of $\text{LiNi}_{0.5-x}\text{Cu}_x\text{Mn}_{1.5-y}\text{Al}_y\text{O}_4$ ($x=0, 0.05, y=0, 0.05$) as 5 V spinel materials. *J Power Sources* 240:95–100
- Liu H, Zhu G, Zhang L, Qu Q, Shen M, Zheng H (2015) Controllable synthesis of spinel lithium nickel manganese oxide cathode material with enhanced electrochemical performances through a modified oxalate co-precipitation method. *J Power Sources* 274:1180–1187
- Luo W (2015) Effect of morphology on the physical and electrochemical properties of the high-voltage spinel cathode $\text{LiNi}_{0.5}\text{Mn}_{1.5}\text{O}_4$. *J Alloy Compd* 636:24
- Lv YZ, Jin YZ, Xue Y, Wu J, Zhang XG, Wang ZB (2014) Electrochemical properties of high-voltage $\text{LiNi}_{0.5}\text{Mn}_{1.5}\text{O}_4$ synthesized by a solid-state method. *RSC Adv* 4:26022–26029
- Manthiram, Chemelewski K, Lee ES (2014) A perspective on the high-voltage $\text{LiNi}_{0.5}\text{Mn}_{1.5}\text{O}_4$ spinel cathode for lithium-ion batteries. *Energy Environ Sci* 7:1339
- Moorhead-Rosenberg Z, Shin DW, Chemelewski KR, Goodenough JB, Manthiram A (2012) Quantitative determination of Mn^{3+} content in $\text{LiMn}_{1.5}\text{Ni}_{0.5}\text{O}_4$ spinel cathodes by magnetic measurements. *Appl Phys Lett* 100:213909
- Mou J, Deng Y, He L, Zheng Q, Jiang N, Lin D (2018) Critical roles of semi-conductive LaFeO_3 coating in enhancing cycling stability and rate capability of 5 V $\text{LiNi}_{0.5}\text{Mn}_{1.5}\text{O}_4$ cathode materials. *Electrochim Acta* 260:101–111
- Park OK, Cho Y, Lee S, Yoo HC, Song HK, Cho J (2011) Who will drive electric vehicles, olivine or spinel? *Energy Environ Sci* 4:1621–1633
- Pieczonka NPW, Liu Z, Lu P, Olson KL, Moote J, Powell BR (2013) Understanding transition-metal dissolution behavior in $\text{LiNi}_{0.5}\text{Mn}_{1.5}\text{O}_4$ high-voltage spinel for lithium ion batteries. *J Phys Chem C* 117:15947–15957
- Ren W, Luo R, Liu ZS, Tan XY, Fu ZY, Liao SJ (2014) Effect of Ni/Mn ratio on the performance of $\text{LiNi}_x\text{Mn}_{2-x}\text{O}_4$ cathode material for lithium-ion battery. *Ionics* 20:1361–1366
- Santhanam R, Rambabu B (2010) Research progress in high voltage spinel $\text{LiNi}_{0.5}\text{Mn}_{1.5}\text{O}_4$ material. *J Power Sources* 195:5442–5451
- Song J, Shin DW, Lu Y, Amos CD, Manthiram A, Goodenough JB (2012) Role of oxygen vacancies on the performance of $\text{Li}[\text{Ni}_{0.5-x}\text{Mn}_{1.5+x}]\text{O}_4$ ($x=0, 0.05, \text{ and } 0.08$) spinel cathodes for lithium-ion batteries. *Chem Mater* 24:3101–3109
- Tong W, Huang Y, Cai Y, Guo Y, Wang X, Jia D, Zong J (2018) Synthesis of hierarchical mesoporous lithium nickel cobalt manganese oxide spheres with high rate capability for lithium-ion batteries. *Appl Surf Sci* 428:1036–1045
- Wan L, Deng Y, Yang C, Xu H, Qin X, Chen G (2015) Ni/Mn ratio and morphology-dependent crystallographic facet structure and electrochemical properties of the high-voltage spinel $\text{LiNi}_{0.5}\text{Mn}_{1.5}\text{O}_4$ cathode material. *RSC Adv* 5:25988–25997
- Xiao J, Chen X, Sushko PV, Sushko ML, Kovarik L, Feng J, Choi D (2012) High performance $\text{LiNi}_{0.5}\text{Mn}_{1.5}\text{O}_4$ spinel controlled by Mn^{3+} concentration and site disorder. *Adv Mater* 24:2109
- Xiao J, Yu X, Zheng J, Zhou Y, Gao F, Chen X, Bai J, Yang X-Q, Zhang J-G (2013) Interplay between two-phase and solid solution reactions in high-voltage spinel cathode material for lithium-ion batteries. *J Power Sources* 242:736–741
- Xue Y, Wang ZB, Yu FD, Zhang Y, Yin GP (2014) Ethanol-assisted hydrothermal synthesis of $\text{LiNi}_{0.5}\text{Mn}_{1.5}\text{O}_4$ with excellent long-term cyclability at high rate for lithium-ion batteries. *J Mater Chem A* 2:4185–4191
- Xue Y, Wang ZB, Zheng LL, Yu FD, Liu BS, Zhou YX (2017) Investigation on spinel $\text{LiNi}_{0.5}\text{Mn}_{1.5}\text{O}_4$ synthesized by MnCO_3 prepared under different conditions for lithium-ion batteries. *ChemistrySelect* 2:4324
- Yao Y, Liu H, Li G, Peng H, Chen K (2014) Multi-shelled porous $\text{LiNi}_{0.5}\text{Mn}_{1.5}\text{O}_4$ microspheres as a 5 V cathode material for lithium-ion batteries. *Mater Chem Phys* 143:867–872
- Yi TF, Hu XG (2007) Preparation and characterization of sub-micro $\text{LiNi}_{0.5-x}\text{Mn}_{1.5+x}\text{O}_4$ for 5 V cathode materials synthesized by an ultrasonic-assisted co-precipitation method. *J Power Sources* 167:185–191
- Yi TF, Mei J, Zhu YR (2016) Key strategies for enhancing the cycling stability and rate capacity of $\text{LiNi}_{0.5}\text{Mn}_{1.5}\text{O}_4$ as high-voltage cathode materials for high power lithium-ion batteries. *J Power Sources* 316:85–105
- Yin C, Zhou H, Yang Z, Li J (2018) Synthesis and electrochemical properties of $\text{LiNi}_{0.5}\text{Mn}_{1.5}\text{O}_4$ for Li-ion batteries by the metal-organic framework method. *ACS Appl Mater Interfaces* 10:13625–13634
- Zhang M, Wang J, Xia Y, Liu Z (2012) Microwave synthesis of spherical spinel $\text{LiNi}_{0.5}\text{Mn}_{1.5}\text{O}_4$ as cathode material for lithium-ion batteries. *J Alloys Compd* 518:68–73
- Zhang Y, Jia D, Tang Y, Huang Y, Pang W, Guo Z, Zhou Z (2018) In situ chelating synthesis of hierarchical $\text{LiNi}_{1/3}\text{Co}_{1/3}\text{Mn}_{1/3}\text{O}_2$ polyhedron assemblies with ultralong cycle life for Li-ion batteries. *Small* 14:1704354
- Zhu Z, Yan H, Zhang D, Li W, Lu Q (2013) Preparation of 4.7 V cathode material $\text{LiNi}_{0.5}\text{Mn}_{1.5}\text{O}_4$ by an oxalic acid-pretreated solid-state method for lithium-ion secondary battery. *J Power Sources* 224:13–19